

Twisted-Eguchi-Kawai model: A reduced model for large- N lattice gauge theory

A. Gonzalez-Arroyo* and M. Okawa

Physics Department, Brookhaven National Laboratory, Upton, New York 11973

(Received 15 December 1982)

We study the large- N reduced model recently proposed by the present authors. This model is a modified version of the Eguchi-Kawai model incorporating twisted boundary conditions. It is shown that the Schwinger-Dyson equations of our model are the same as in the infinite-lattice theory provided $[U(1)]^4$ symmetry is not spontaneously broken. We study the model at strong coupling, weak coupling, and intermediate coupling using analytical and Monte Carlo techniques. At weak coupling, it is shown that for a particular choice of twist, $[U(1)]^4$ symmetry is not broken and we prove how one recovers usual planar perturbation theory. Monte Carlo data for χ ratios show striking agreement with Wilson-theory results.

I. INTRODUCTION

The $N \rightarrow \infty$ limit¹ of lattice gauge theories² has been the subject of many interesting studies in recent years. The ultimate hope is to be able to solve the theory in this limit. However, this aim has not been achieved at present, despite the remarkable simplifications already discovered. It is known that only planar diagrams survive in this limit,¹ and that the planar perturbative series is convergent.^{3,4} Nevertheless, summing this series explicitly has only been achieved for the two-dimensional continuum theory.⁵ On the lattice the $N \rightarrow \infty$ limit of two-dimensional $SU(N)$ Yang-Mills theories has also been solved⁶ using the techniques of Ref. 7. Another important simplification that takes place in the $N \rightarrow \infty$ limit is factorization.^{8,9} This property allows one to obtain closed equations for Wilson loops¹⁰ and leads to the fundamental concept of a master field.⁹

Recently, a new important result has been developed. A fundamental reduction of degrees of freedom takes place in the $N \rightarrow \infty$ limit. One can omit the space-time dependence of the gauge fields. The key observation was made by Eguchi and Kawai¹¹ who showed that the loop equations¹² of the infinite-lattice Wilson theory coincide with those of the Eguchi-Kawai (EK) model. The partition function of the latter model is that of a one-site Wilson theory with periodic boundary conditions.

The derivation of Eguchi and Kawai was based on an important assumption. In order for the reduction to hold vacuum expectation values of traces of open loops must vanish. This is guaranteed provided the $[U(1)]^4$ symmetry of the action is not broken spontaneously. It was pointed out that this symmetry is probably broken at weak coupling.¹³ This fact

was known even before the work of Eguchi and Kawai.¹⁴ Since then Monte Carlo simulations have shown that this in fact takes place.^{13,15}

To save the idea of the reduction of degrees of freedom Bhanot, Heller, and Neuberger¹³ proposed the quenched-Eguchi-Kawai (QEK) model. In this model the eigenvalues of the link matrices are quenched, i.e., treated as classical variables. Physical quantities are averaged over all values of the eigenvalues with a uniform distribution. It was argued that the QEK model coincides with the usual EK model at strong coupling where $[U(1)]^4$ symmetry is not broken. At weak coupling it is the former, not the latter, which behaves properly. Monte Carlo simulations have been presented which substantiate this claim.^{16,17}

Parisi proposed a general procedure for quenching,¹⁸ which applies for all matrix models, and argued that a similar procedure can be used in the continuum. Several authors¹⁹⁻²¹ incorporated this prescription into gauge theories. In particular, Gross and Kitazawa²¹ showed that the Parisi prescription can be suitably modified and agrees with the QEK model. In addition, they show how one obtains planar perturbation theory in the weak-coupling region. When applied to the continuum theory, the quenching prescription provides a gauge-invariant cutoff regularization.

Different derivations²² and applications²³ of the quenched reduction of degrees of freedom have been discovered recently. At the same time, other authors have explored different solutions.²⁴

Recently, the present authors²⁵ proposed a very simple alternative: the twisted-Eguchi-Kawai (TEK) model. The main idea is to consider the EK model with twisted boundary conditions²⁶ rather than purely periodic conditions. It is known that at

weak coupling the behavior of the partition function differs significantly between the twisted case²⁷ and the purely periodic case.¹⁴ It is then possible to expect that in the TEK model one excludes $[U(1)]^4$ symmetry breaking at weak coupling. Our preliminary study of the TEK model²⁵ supported this belief.

In the present paper we will study the TEK model in detail. In Sec. II the model is presented and it is shown that the proof of Eguchi and Kawai applies to our case as well. Consequently, the loop equations of the TEK model are equivalent to those of the infinite-lattice Wilson theory, under the assumption that $[U(1)]^4$ symmetry is not spontaneously broken.

In Sec. III we show that in the strong-coupling region the TEK model behaves in the same way as the EK model. Therefore, if the latter model is equivalent to the infinite-lattice theory, as is generally assumed, so is the former. To quantify the approach to the $N \rightarrow \infty$ limit in this region, we present some finite- N corrections for Wilson loops.

In Sec. IV we study the zero-action solutions which dominate the path integral at weak coupling. A comparison of different twists is made. We conclude that for a particular choice of twist (symmetric twist) all traces of open loops are zero in the $N \rightarrow \infty$ limit, as required for the equivalence of the loop equations. The symmetric-twist configuration demands $N = L^2$ (L an integer). No solutions of the type given in Refs. 27 and 28 apply to our case. For $L = 2$ solutions were found in Ref. 25. In the present paper we give the solution for arbitrary L .

In Sec. V we study perturbation theory for the symmetric-twist TEK model. We show how planar perturbation theory emerges. The leading finite- N corrections correspond to the finite-size effects on an L^4 lattice. We argue that a similar prescription can be used in any matrix model.

In Sec. VI we study the behavior of the model using Monte Carlo methods. The data show how traces of open loops are zero throughout the whole range of the coupling constant, in agreement with our strong- and weak-coupling considerations. The internal energy shows the expected weak- and strong-coupling behavior. A first-order phase transition is seen at $\beta/N = 0.36$, as expected for the infinite-lattice Wilson theory in the $N \rightarrow \infty$ limit.²⁹ Larger Wilson loops are also studied for $SU(36)$ and the χ ratios show striking resemblance to those of the Wilson theory³⁰ on a 6^4 lattice.

Finally, in Sec. VII the concluding remarks are presented. We comment on the two-dimensional model and show the comparison of our data with the results of Gross and Witten.⁶ Some prospects for future work are stated.

II. LOOP EQUATIONS

Here we define the TEK model and show that the Schwinger-Dyson equations of our model agree with those of the infinite-lattice Wilson theory. A proof of this fact was already given in Ref. 25, for a particular choice of twist.

The partition function of the usual Wilson theory is given by

$$\begin{aligned} Z_W &= \int \prod_l dU(l) \exp \left\{ -\beta \sum_P \text{Tr}[I - U(P)] \right\} \\ &= \int \prod dU e^{-\beta S(U)}, \end{aligned} \quad (2.1)$$

where l stands for link, P for plaquette, and I is the $N \times N$ unit matrix. $U(P)$ is the ordered product of the $SU(N)$ link variables $U(l)$ along the contour of the plaquette P . The vacuum expectation value of the Wilson loop $W(C)$ is given by the standard formula

$$\langle W(C) \rangle = \int \prod dU \text{Tr} \left[\prod_{l \in C} U(l) \right] e^{-\beta S(U)} / Z_W. \quad (2.2)$$

To obtain the twisted model, we first apply the transformation

$$U(l) \rightarrow U'(l) = Z(l)U(l), \quad Z(l) \in Z_N \quad (2.3)$$

to the partition function (2.1). Under this transformation $U(P)$ transforms as

$$\begin{aligned} U(P) &\rightarrow U'(P) = Z(P)U(P), \\ Z(P) &\equiv \prod_{l \in \partial P} Z(l), \end{aligned} \quad (2.4)$$

where ∂P denotes the boundary of the plaquette P . $Z(P)$ satisfies the following Bianchi identities for any cube C ,

$$\prod_{P \in \partial C} Z(P) = 1. \quad (2.5)$$

The measure of integration is invariant under the transformation (2.3) and Eq. (2.1) becomes

$$Z_W = \int \prod_l dU(l) \exp \left\{ -\beta \sum_P \text{Tr}[I - Z(P)U(P)] \right\}. \quad (2.6)$$

In terms of the new variables the Wilson loops are expressed as

$$\begin{aligned} \prod_{l \in C} U'(l) &= \prod_{l \in C} Z(l)U(l) \\ &= \left[\prod_{P \in S} Z(P) \right] \prod_{l \in C} U(l), \end{aligned} \quad (2.7)$$

where S is the minimal surface with contour C . Notice that in Eqs. (2.6) and (2.7), $Z(l)$ appear only in the combination $Z(P)$.

Furthermore, $Z(P)$ are arbitrary provided that they satisfy identities (2.5). For our purpose, however, we only consider the following translation-invariant $Z(P)$ configuration:

$$Z(P) = Z_{\mu\nu}, \quad Z_{\mu\nu} = Z_{\nu\mu}^* \quad (2.8)$$

In this case $Z(P)$ depends on the orientation (μ, ν) of the plaquette P , but not on the space-time loca-

tion. The configuration (2.8) is possible because it satisfies (2.5). The corresponding transformation (2.3) is determined up to Z_N gauge transformations.

Using the particular representation (2.6)–(2.8) of the usual Wilson theory, we reduce the model by neglecting the space-time dependence of the link variables

$$U(l) \equiv U_\mu(x) \rightarrow U_\mu \quad (2.9)$$

In this way the partition function (2.6) becomes

$$Z_{W \rightarrow Z_{\text{TEK}}} = \int \prod_\mu dU_\mu \exp \left[-\beta \sum_{\mu \neq \nu=1}^d \text{Tr}(I - Z_{\mu\nu} U_\mu U_\nu U_\mu^\dagger U_\nu^\dagger) \right] \quad (2.10)$$

and the Wilson loop is given by

$$\left[\prod_{P \in S} Z(P) \right] \text{Tr}[U_\mu(x) U_\nu(x + \hat{\mu}) \cdots U_\sigma(x - \hat{\sigma})] \rightarrow \left[\prod_{\mu\nu} Z_{\mu\nu}^{NP_{\mu\nu}} \right] \text{Tr}(U_\mu U_\nu \cdots U_\sigma), \quad (2.11)$$

where $NP_{\mu\nu}$ is the number of plaquettes in the (μ, ν) direction on the surface S and d is the space-time dimension. Equations (2.10) and (2.11) define our reduced TEK model.²⁵ Notice that this model is just the one-site Wilson model with twisted boundary conditions²⁶ specified by $Z_{\mu\nu}$.

The action (2.10) is invariant under the $(Z_N)^d$ symmetry $U_\mu \rightarrow Z_\mu U_\mu$ with $Z_\mu \in Z_N$. In the $N \rightarrow \infty$ limit this symmetry becomes $[U(1)]^d$. The original Eguchi-Kawai model¹¹ corresponds to taking all $Z_{\mu\nu} = 1$. Each twist $Z_{\mu\nu}$ can be labeled by a set of integers $n_{\mu\nu}$ (modulo N):

$$Z_{\mu\nu} = \exp(2\pi i n_{\mu\nu}/N) \quad (2.12)$$

Now following the arguments of Ref. 11, we will show that the Schwinger-Dyson equations of the Wilson loop (2.11) in the TEK model coincide with those of the usual Wilson theory under the assumption that $[U(1)]^d$ symmetry is not spontaneously broken.

Consider the following expression in the Wilson theory (2.6):

$$\left[\prod_{P \in S} Z(P) \right] \langle \text{Tr}[\lambda^a U_\mu(x) U_\nu(x + \hat{\mu}) \cdots U_\sigma(x - \hat{\sigma})] \rangle, \quad (2.13)$$

where λ^a ($a = 1$ to $N^2 - 1$) denotes a generator of the Lie algebra of $SU(N)$. By making an infinitesimal change of variables

$$U_\mu(x) \rightarrow (1 + i\epsilon\lambda^a) U_\mu(x), \quad (2.14)$$

we obtain

$$\left[\prod_{P \in S} Z(P) \right] \langle \text{Tr}[\lambda^a \lambda^a U_\mu(x) U_\nu(x + \hat{\mu}) \cdots U_\sigma(x - \hat{\sigma})] \rangle + \left[\prod_{P \in S} Z(P) \right] \langle \text{Tr}[\lambda^a U_\mu(x) U_\nu(x + \hat{\mu}) \cdots U_\sigma(x - \hat{\sigma})] \delta S^a \rangle = 0, \quad (2.15)$$

where

$$\delta S^a = \sum_{\rho \neq \mu} \beta \{ Z_{\mu\rho} \text{Tr}[\lambda^a U_\mu(x) U_\rho(x + \hat{\mu}) U_\mu^\dagger(x + \hat{\rho}) U_\rho^\dagger(x)] - Z_{\rho\mu} \text{Tr}[\lambda^a U_\rho(x) U_\mu(x + \hat{\rho}) U_\rho^\dagger(x + \hat{\mu}) U_\mu^\dagger(x)] \}. \quad (2.16)$$

After summing over a and making use of the identity

$$\sum_a \lambda_{ij}^a \lambda_{kl}^a = \frac{1}{2} \delta_{ij} \delta_{jk} + O\left(\frac{1}{N}\right), \quad (2.17)$$

we arrive at the formula

$$\left[\prod_{P \in S} Z(P) \right] \left\langle \text{Tr} \prod_{l \in C} U(l) \right\rangle + \frac{\beta}{N} \sum_{\rho \neq \mu} \left[\prod_{P \in S'_\rho} Z(P) \right] \left\langle \text{Tr} \prod_{l \in C'_\rho} U(l) \right\rangle - \frac{\beta}{N} \sum_{\rho \neq \mu} \left[\prod_{P \in S''_\rho} Z(P) \right] \left\langle \text{Tr} \prod_{l \in C''_\rho} U(l) \right\rangle = 0, \quad (2.18)$$

where the contours C , C'_ρ , and C''_ρ are illustrated in Fig. 1. The labels S , S'_ρ , and S''_ρ specify the minimum surfaces with contours C , C'_ρ , and C''_ρ , respectively. Notice that Eqs. (2.18) are the ordinary loop equations of the Wilson theory supplemented with the Z factors according to Eq. (2.7).

When the link $U_\mu(x)$ appears more than once in the original contour C , we obtain additional terms in Eqs. (2.15) and (2.18). For example, if the link $U_\mu(x)$ occurs twice in the contour C as in Fig. 2, we have an additional term

$$- \left[\prod_{P \in S} Z(P) \right] \left\langle \left[\text{Tr} \prod_{l \in C_1} U(l) \right] \left[\text{Tr} \prod_{l \in C_2} U(l) \right] \right\rangle = - \left[\prod_{P \in S_1} Z(P) \right] \left[\prod_{P \in S_2} Z(P) \right] \left\langle \text{Tr} \prod_{l \in C_1} U(l) \right\rangle \left\langle \text{Tr} \prod_{l \in C_2} U(l) \right\rangle \quad (2.19)$$

in the right-hand side of Eq. (2.18), where C_1 and C_2 are given in Fig. 3. To derive the right-hand side of Eq. (2.19) we used the factorization property of disconnected loops in the large- N limit.^{8,9} Following Ref. 11, we call these terms "source terms."

Next we discuss the Schwinger-Dyson equations

in the TEK model. If we repeat the derivations, we find the same equations except for the appearance of extra source terms which arise because all link variables in the same direction are identified. For example, consider the following quantity:

$$\left[\prod_{P \in S} Z(P) \right] \left\langle \text{Tr} [\lambda^a U_\mu(x) U_\nu(x + \hat{\mu}) \cdots U_\lambda(y - \hat{\lambda}) U_\mu(y) \cdots U_\rho(x - \hat{\rho})] \right\rangle. \quad (2.20)$$

In the reduced model $U_\mu(x)$ and $U_\mu(y)$ are identified even for $y \neq x$. Thus, we have additional source terms,

$$\left[\prod_{P \in S} Z(P) \right] \left\langle \text{Tr} (U_\mu U_\nu \cdots U_\lambda) \right\rangle_{\text{TEK}} \left\langle \text{Tr} (U_\mu \cdots U_\rho) \right\rangle_{\text{TEK}}. \quad (2.21)$$

The sequences $(\mu, \nu, \dots, \lambda)$ and (μ, \dots, ρ) correspond to open paths C_1 and C_2 joining x and y :

$$\begin{aligned} C_1 &= (x, x + \mu, \dots, y - \lambda, y), \\ C_2 &= (y, y + \mu, \dots, x - \rho, x), \end{aligned} \quad (2.22)$$

in the usual Wilson theory.

We note that $U_\mu U_\nu \cdots U_\lambda$ and $U_\mu \cdots U_\rho$ are not invariant under the transformation $U_\rho \rightarrow e^{i\theta} U_\rho$ since there exists at least one direction ρ for which U_ρ and U_ρ^\dagger appear different number of times. Thus if the $[U(1)]^d$ symmetry is not spontaneously broken we have

$$\left\langle \text{Tr} (U_\mu U_\nu \cdots U_\lambda) \right\rangle_{\text{TEK}} = \left\langle \text{Tr} (U_\mu \cdots U_\rho) \right\rangle_{\text{TEK}} = 0 \quad (2.23)$$

and the Schwinger-Dyson equations obeyed by (2.7) and (2.11) coincide.

We have shown that if $[U(1)]^d$ symmetry is not spontaneously broken the Schwinger-Dyson equations of the TEK model [Eq. (2.10)] coincide with those derived from our particular representation (2.6) of the Wilson theory. Assuming that these

equations specify the theory uniquely we conclude

$$\begin{aligned} \left[\prod_{P \in S} Z(P) \right] \left\langle \text{Tr} \prod_{l \in C} U(l) \right\rangle \\ = \left[\prod_{\mu\nu} Z_{\mu\nu}^{NP} \right] \left\langle \text{Tr} \prod_{\rho} U_\rho \right\rangle_{\text{TEK}}, \end{aligned} \quad (2.24)$$

where the left and right vacuum expectation values are calculated using (2.6) and (2.10), respectively. One can reexpress this result in terms of the usual partition function of Wilson's theory,

$$\langle W(C) \rangle = \left[\prod_{\mu\nu} Z_{\mu\nu}^{NP} \right] \left\langle \text{Tr} \prod_{\rho} U_\rho \right\rangle_{\text{TEK}}, \quad (2.25)$$

where $\langle W(C) \rangle$ is now defined as in (2.2).

III. STRONG-COUPLING BEHAVIOR

In the strong-coupling region the $[U(1)]^d$ symmetry is not broken in any finite order of the strong-coupling expansion in the EK model. Then the equivalence of the Schwinger-Dyson equations implies that the EK model is identical to the infinite-

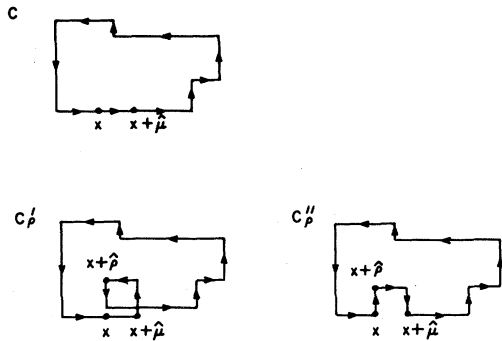


FIG. 1. Contours appearing in the Schwinger-Dyson equations.

lattice Wilson theory provided the equations specify the theory uniquely. In this section we will show that if this assumption is true for the EK model, the TEK model is also equivalent to Wilson's theory in the strong-coupling region.

Consider first the vacuum diagrams. In the infinite-lattice Wilson theory, the set of strong-coupling diagrams corresponds to the set of all closed surfaces on the lattice. In the $N \rightarrow \infty$ limit only the planar surfaces contribute. On the other hand, in the Eguchi-Kawai model there are many more terms which can contribute due to the periodicity of boundary conditions. For example, a single plaquette is in this case a closed surface (two-dimensional torus). In order that the EK model has the same strong-coupling expansion as the Wilson theory, these extra terms must vanish in the $N \rightarrow \infty$ limit. Explicit calculations will be given later which agree with this fact. The underlying reason for the vanishing of the extra terms in the strong-coupling expansion of the EK model is probably the fact that they correspond to nonplanar surfaces. This is clear in the example mentioned previously.

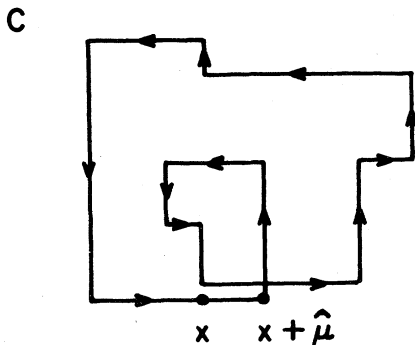


FIG. 2. A contour in which $U_\mu(x)$ appears twice.

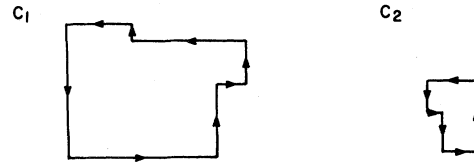


FIG. 3. Contours contributing to the source terms.

Next we see what happens in the case of the TEK model. First of all, notice that the presence of a twist does not affect the link integrations. Therefore, the set of diagrams which survive in the $N \rightarrow \infty$ limit is the same as in the EK model. This set was assumed to be given by all surviving vacuum diagrams in Wilson's theory. Now we must prove that the result for each of these diagrams coincides in the EK and TEK models.

In general, the effect of a twist is to multiply the value of the diagram in the EK model by a phase. This phase is the product of all $Z_{\mu\nu}$ factors for each plaquette of the surface. However, for the surviving diagrams in the $N \rightarrow \infty$ limit the product of these factors is equal to 1, and consequently the EK and TEK models give identical results. To see why this happens, consider first the case of a cube. In this example our claim is a consequence of the Bianchi identities (2.5). For a more complicated planar surface the result can be extended due to the Abelian nature of the $Z_{\mu\nu}$ factors. In other words, the phase factor of a given closed surface measures the Z_N magnetic flux coming out of this surface. If the surface is closed in the infinite lattice the phase factor must be 1 due to the absence of Z_N magnetic monopoles (2.5). On the other hand, nonleading diagrams can in principle differ for the EK model and TEK model, by a multiplicative phase factor.

Extension of this result to the strong-coupling behavior of Wilson loops $\langle W(C) \rangle$ is easy to obtain. In this case the set of diagrams is given by all open surfaces with contour on the particular Wilson loop. Considering any such surface and the minimal surface with contour C we form a closed surface and the previous result can be applied. In this context, notice that the Wilson loop in the TEK model must be multiplied by the appropriate $Z_{\mu\nu}$ factors as shown in Eq. (2.11).

To conclude this section we will present the first coefficients in the strong-coupling expansion of the vacuum expectation values of several Wilson loops in the EK model. As mentioned previously, non-leading terms can differ from those in the TEK model as well as for different twist configurations. Our results are shown in Table I. The magnitude of nonleading $1/N$ corrections is seen to be small for the values of N considered in Sec. VI.

TABLE I. Leading terms in the strong-coupling expansion for vacuum expectation values of $I \times J$ Wilson loops $\langle W(I, J) \rangle$ in the EK model.

$\langle W(1,1) \rangle$	$\frac{1}{N} + \frac{N^4 + 10N^2 - 6}{N(N^2 - 1)} \frac{\beta}{N}$
$\langle W(1,2) \rangle$	$\frac{2}{N}$
$\langle W(2,2) \rangle$	$\frac{3N^2 - 4}{N(N^2 - 1)} + \frac{40N^4 - 116N^2 + 32}{N(N^2 - 1)(N^2 - 4)} \frac{\beta}{N}$
$\langle W(3,2) \rangle$	$\frac{4N^2 - 6}{N(N^2 - 1)}$
$\langle W(3,3) \rangle$	$\frac{5N^2 - 9}{N(N^2 - 1)}$

IV. ZERO-ACTION SOLUTIONS

The leading behavior of all the observables at weak coupling ($\beta \rightarrow \infty$) is dominated by the configurations $U_\mu^{(0)}$ that minimize the action

$$S_{\min} = \sum_{\mu, \nu} (N - Z_{\mu\nu} \text{Tr} U_\mu^{(0)} U_\nu^{(0)} U_\mu^{(0)\dagger} U_\nu^{(0)\dagger}). \quad (4.1)$$

In particular any loop (open or closed) behaves as

$$\langle \text{Tr}(U_{\mu_1} \cdots U_{\mu_n}) \rangle_{\beta \rightarrow \infty} = \text{Tr}(U_{\mu_1}^{(0)} \cdots U_{\mu_n}^{(0)}). \quad (4.2)$$

In the presence of twisted boundary conditions it is not always possible to saturate the bound $S_{\min} \geq 0$. A necessary²⁸ and sufficient³¹ condition is given by

$$\frac{1}{4} n_{\mu\nu} \tilde{n}_{\mu\nu} = \sigma N, \quad (4.3)$$

where σ is an integer and

$$\tilde{n}_{\mu\nu} = \frac{1}{2} \epsilon^{\mu\nu\rho\sigma} n_{\rho\sigma} \quad (4.4)$$

is the dual of $n_{\mu\nu}$. If relation (4.3) is not satisfied, solutions have a rational Pontryagin number and the action is bounded from below by a positive quantity. In the continuum one can obtain this quantity in terms of the Pontryagin index. On the lattice an equivalent relation is not known to the authors, but Monte Carlo simulations²⁵ show that condition (4.3) is still required. From now on, we will restrict ourselves to twists satisfying (4.3).

The problem of finding zero-action configurations with twists was first studied in Refs. 27 and 32. One must find 4 ($=d$) $SU(N)$ matrices $U_\mu^{(0)}$ satisfying

$$U_\mu^{(0)} U_\nu^{(0)} = \exp \left[\frac{2\pi i}{N} n_{\nu\mu} \right] U_\nu^{(0)} U_\mu^{(0)}. \quad (4.5)$$

Recently 't Hooft²⁸ proved that, provided N is not a multiple of a prime number squared, solutions exist, and he gave a recipe to construct them. It is worthwhile to recall this explicit construction.

Let us introduce $N \times N$ matrices P_N and Q_N as follows:

$$P_N = \begin{pmatrix} 0 & 1 & & \\ & 0 & 1 & \\ & & \ddots & \ddots \\ & & & 0 & 1 \\ 1 & & & & 0 \end{pmatrix}, \quad (4.6)$$

$$Q_N = e^{\pi i(1-N)/N} \begin{pmatrix} 1 & & & \\ & e^{2\pi i/N} & & \\ & & \ddots & \\ & & & e^{2\pi i(N-1)/N} \end{pmatrix}.$$

They are $SU(N)$ matrices satisfying

$$P_N Q_N = \exp(2\pi i/N) Q_N P_N. \quad (4.7)$$

Now one can show²⁸ that whenever N is not a multiple of a prime number squared and Eq. (4.3) is verified, there exist integers s_μ and t_μ ($\mu = 1$ to d) such that

$$U_\mu^{(0)} = P_N^{s_\mu} Q_N^{t_\mu} \quad (4.8)$$

satisfies (4.5).

The above requirement on the number of colors is a consequence of the particular ansatz (4.8). In Ref. 25 the authors found new solutions to (4.5) of a different type, and other new solutions will be given later (see also Ref. 32).

We now want to focus on the properties of these configurations. First of all notice that

$$\text{Tr} P_N = \text{Tr} Q_N = 0. \quad (4.9)$$

Furthermore, any matrix of the form $P_N^{s_\mu} Q_N^{t_\mu}$ is traceless, provided s_μ or t_μ are not multiples of N . Consequently, several open paths will automatically have zero expectation values at weak coupling. This property is not a consequence of 't Hooft's ansatz (4.8). It depends only on the twist configuration. In general we have the following result.

Theorem. Given any two unitary matrices A, B such that $AB = e^{i\delta} BA$ with $\delta \neq 2\pi k$, then $\delta = 2\pi n/N$ and $\text{Tr}(AB) = \text{Tr} A = \text{Tr} B = 0$.

Therefore, let us consider general $SU(N)$ matrices $U_\mu^{(0)}$ satisfying (4.5). By multiplying these matrices any number of times, we generate new matrices which form the basis of a matrix algebra. Any two elements of this kind A, B satisfy $AB = e^{i\delta(A,B)} BA$ and are, therefore, traceless provided δ is not a multiple of 2π . A general element of this basis has the form

$$U(k) = (U_0^{(0)})^{k_0} (U_1^{(0)})^{k_1} (U_2^{(0)})^{k_2} (U_3^{(0)})^{k_3}, \quad (4.10)$$

where k are integers and specify the coordinates of a

point in a four-dimensional lattice. The matrix $U(k)$ then corresponds to a loop joining the origin to the point $k \equiv (k_\mu)$. Any other loop with the same end points will be given by $e^{i\delta(c)}U(k)$.

The requirement that symmetry is not broken at weak coupling demands $\text{Tr}U(k)=0$ for all open loops ($k \neq 0$). This condition will be automatically guaranteed provided that $U(k)$ does not commute with some other element of the basis.

Then we are lead naturally to the study of those elements of the basis which commute with the whole algebra. A necessary and sufficient condition for this is that it commutes with the generators:

$$[U(k), U_\mu^{(0)}] = 0 \text{ for all } \mu = 1 \text{ to } 4. \tag{4.11}$$

Using relation (4.5) one obtains the corresponding condition on the k_μ ,

$$k_\mu n_{\mu\nu} = q_\nu N, \tag{4.12}$$

where q are integers.

To solve this equation it is natural to distinguish two cases depending on whether σ appearing in (4.3) is zero or not. In the former case one can obtain solutions even for $q_\nu = 0$. These solutions are

$$k_\mu = \tilde{n}_{\mu\rho} s_\rho, \tag{4.13}$$

where s are not necessarily integers but k are.

For $\sigma \neq 0$ the solution is easily obtained, noticing that

$$\tilde{n}_{\mu\nu} n_{\rho\nu} = \sigma N \delta_{\mu\rho}. \tag{4.14}$$

We get

$$\sigma k_\mu = \tilde{n}_{\mu\nu} q_\nu. \tag{4.15}$$

Thus, for any finite N there are always some open paths $U(k)$ given by (4.13) and (4.15) whose trace is not forced to be zero at weak coupling. In fact, if the algebra is irreducible $U(k)$ is a multiple of the identity and the trace is nonzero. However, as we will now show, it is possible to choose $n_{\mu\nu}$ such that in the $N \rightarrow \infty$ limit all $U(k)$ are traceless.

Consider the case that $N=L^2$ (L an integer) and choose the following "symmetric twist" configuration

$$n_{\mu\nu} = L \text{ for } \mu > \nu. \tag{4.16}$$

Relation (4.3) is satisfied with $\sigma=1$ and the only set k_μ satisfying (4.15) is given by the multiples of L . The algebra generated by the solutions can be labeled by the points of an L^4 periodic lattice. All open paths on this lattice have zero trace. As $N=L^2$ goes to infinity the lattice becomes infinite and all open paths will have zero trace.

An important advantage in our construction is that the finite- N corrections come out as those of a finite L^4 lattice. Later on, we will see that this relationship is further substantiated.

We still have to show that one can find zero-action solutions for the symmetric-twist configuration (4.16). As mentioned previously there are no solutions of 't Hooft type (4.8). For $L=2$ ($N=4$) solutions were reported in Ref. 25. They are given by the Dirac matrices $U_\mu^{(0)} = \gamma_\mu$. The basis of the Clifford algebra corresponds to the points of a 2^4 periodic lattice. For $L > 2$ one can obtain generalizations of these solutions. An explicit representation is as follows:

$$\begin{aligned}
 U_0^{(0)} &= \begin{pmatrix} 0 & I & & & \\ & 0 & I & & \\ & & 0 & \ddots & \\ & & & 0 & I \\ I & & & & 0 \end{pmatrix}, \\
 U_1^{(0)} &= \begin{pmatrix} P_L & & & & \\ & P_L \exp(2\pi i/L) & & & \\ & & \ddots & & \\ & & & P_L \exp[2\pi i(L-1)/L] & \\ & & & & \end{pmatrix}, \\
 U_2^{(0)} &= \begin{pmatrix} P_L Q_L & & & & \\ & P_L Q_L \exp(2\pi i/L) & & & \\ & & \ddots & & \\ & & & P_L Q_L \exp[2\pi i(L-1)/L] & \\ & & & & \end{pmatrix}, \\
 U_3^{(0)} &= \begin{pmatrix} Q_L & & & & \\ & Q_L \exp(2\pi i/L) & & & \\ & & \ddots & & \\ & & & Q_L \exp[2\pi i(L-1)/L] & \\ & & & & \end{pmatrix}.
 \end{aligned} \tag{4.17}$$

They are built in blocks of $L \times L$ matrices involving I , Q_L , and P_L . In the particular case $L=2$ one obtains a representation of the Dirac matrices.

The set of matrices $U_\mu^{(0)}$ of Eq. (4.17) generate an $N^2=L^4$ dimensional algebra which is a natural generalization of the Clifford algebra.

In the following sections we will restrict ourselves to the symmetric-twist configuration (4.16). Our first concern will be to study perturbation theory in the TEK model.

V. PERTURBATION THEORY

Let us consider the perturbative expansion around the zero-action solution (4.17) found in the previous section. To simplify notation let us refer to these solutions as γ_μ and let U_μ be the link variables.

The first step is to change variables in the path integral in the following way,

$$U_\mu = V_\mu \gamma_\mu. \quad (5.1)$$

In terms of the new variables V_μ the partition function of the twisted-Eguchi-Kawai model becomes

$$Z_{\text{TEK}} = \int dV_\mu \exp \left[-\beta \sum_{\mu,\nu} \text{Tr}(I - V_\mu \gamma_\mu V_\nu \gamma_\nu^\dagger V_\mu^\dagger \gamma_\mu^\dagger V_\nu^\dagger) \right]. \quad (5.2)$$

Notice that $Z_{\mu\nu}$ disappears from the action. Its form can be obtained from the infinite-lattice action (2.1) by applying the following generalized Parisi prescription:

$$V_\nu(n+\mu) \rightarrow \gamma_\mu V_\nu(n) \gamma_\mu^\dagger. \quad (5.3)$$

In a similar fashion, under the change of variables (5.1), Wilson loops can be reexpressed as follows:

$$\prod_{p \in S(C)} Z(p) \prod_{l \in C} U(l) = \tilde{W}(C), \quad (5.4)$$

where $\tilde{W}(C)$ is obtained from the usual infinite-lattice loop by applying relation (5.3).

Before expanding V_μ around the unit matrix, one must fix the zero modes of the action. This can be done in the standard Faddeev-Popov fashion.³³ For definiteness we choose the natural generalization of the Feynman gauge on the lattice after applying the prescription of Eq. (5.3):

$$G_F = \sum_\mu (\gamma_\mu^\dagger V_\mu \gamma_\mu - V_\mu), \quad (5.5)$$

$$S_{\text{gf}} = 2 \text{Tr}(G_F G_F^\dagger).$$

The corresponding ghost interaction is given by

$$S_{\text{gh}} = \text{Tr} \left[\bar{\eta} \sum_\mu [\gamma_\mu^\dagger [\omega, V_\mu \gamma_\mu]] \right]. \quad (5.6)$$

Finally we can expand $V_\mu = \exp(iQ_\mu)$ and express the Haar measure as an integral over Q_μ . The Jacobian can be written as $\exp(-S_{\text{measure}})$. As usual, neglecting some nonperturbative effects one can extend the integration region to arbitrary traceless Hermitian matrices.

This lengthy procedure is the standard one and the final resulting action in our case is obtained by

application of rule (5.3) to the usual action. In particular, the bilinear term in the exponent is given by

$$-2\beta \sum_{\mu,\nu} \text{Tr}(\gamma_\mu Q_\nu \gamma_\mu^\dagger - Q_\nu)^2. \quad (5.7)$$

Usually one expands $Q_\mu = \sum_a Q_\mu^a \lambda^a$ where λ^a are the generators of the Lie algebra,

$$\text{Tr}(\lambda^a \lambda^b) = \frac{1}{2} \delta^{ab}, \quad (5.8)$$

and Q_μ^a are some real coefficients. However, it is more convenient to use the following basis of the Lie algebra,

$$A(q) = \gamma_0^{k_0} \gamma_1^{k_1} \gamma_2^{k_2} \gamma_3^{k_3}, \quad (5.9)$$

where

$$k_\nu = \frac{1}{L} \tilde{n}_{\mu\nu} q_\mu \quad (5.10)$$

and q_μ are integers $1 \leq q_\mu \leq L$ (excluding $q_\mu = L$ for all μ). These are

$$L^4 - 1 = N^2 - 1 \quad (5.11)$$

traceless unitary and linearly independent matrices and satisfy the following property:

$$\gamma_\mu A(q) \gamma_\mu^\dagger = \exp \left[\frac{2\pi i}{L} q_\mu \right] A(q). \quad (5.12)$$

Now we can express Q_μ in terms of these matrices

$$Q_\mu = \frac{1}{N^2} \sum_{q_\mu=1}^L Q_\mu(q) A(q), \quad (5.13)$$

where $Q_\mu(q)$ are complex coefficients obeying

$$Q_\mu^*(q) = Q_\mu(L-q) \exp \left[-\frac{2\pi i}{N} \sum_{\mu>\nu} n_{\nu\mu} k_\mu k_\nu \right] \quad (5.14)$$

and $Q_\mu(0) = Q_\mu(L) = 0$ since Q_μ is traceless.

It is evident from this construction that q_μ plays the role of lattice momenta and $Q_\mu(q)$ are the Fourier coefficients of a lattice field. Furthermore, momenta are conserved at the vertices according to the rule

$$\text{Tr}[A(q_1) \cdots A(q_n)] = N\delta \left[\sum_i q_i \right] \exp \left[\frac{2\pi i}{N} \sum_{i < j} \langle k_i | k_j \rangle \right], \quad (5.15)$$

where

$$\langle k | q \rangle = \sum_{\mu > \nu} k_\mu q_\nu n_{\nu\mu}, \quad (5.16)$$

and the δ function is defined modulo L .

Let us look first at the kinetic term

$$-\frac{2\beta}{N^3} \sum_{q_\mu=1}^L 2 \sum_{\mu} \left[1 - \cos \frac{2\pi q_\mu}{L} \right] \sum_{\nu} Q_\nu(q) Q_\nu^*(q). \quad (5.17)$$

From this expression one concludes that the propagator is equal to the propagator of an L^4 periodic lattice. An analogous result holds for the propagator of the ghost field. As a consequence of this fact, when $N \rightarrow \infty$ the leading behavior of Wilson loops is the same as for an infinite-lattice theory, and finite- N effects correspond to finite-size effects of an L^4 lattice.

The vertices of our theory have the same momentum dependence as the $SU(N)$ Yang-Mills theory on an L^4 lattice. The difference between the theories is given by the group factors on the vertices. In our case they are momentum-dependent phases as seen in Eq. (5.15). For example, $\text{Tr}(\lambda^a \lambda^b \lambda^c)$ is replaced by

$$\text{Tr}[A(q_1)A(q_2)A(q_3)]. \quad (5.18)$$

The ordering of the matrices within one trace is essential, up to cyclic permutations. Later on we will see how the phases in (5.15) play a crucial role in selecting planar diagrams for large N .

In the $N \rightarrow \infty$ limit one can rescale the momentum variables in the form $\phi_\mu = 2\pi q_\mu / L$ and the momentum sum becomes

$$\int_0^{2\pi} \frac{d\phi_\mu}{2\pi}. \quad (5.19)$$

At the same time it is convenient to redefine

$$Q(\phi) \rightarrow (N/\beta)^{1/2} Q(\phi). \quad (5.20)$$

In this way all vertices have the usual coupling constant dependence and N disappears from everywhere

except from the phases sitting at the vertices. In terms of the new variables these phases become

$$\exp \left[\frac{i}{2\pi} \sum_{i > j} \langle \phi_i | \phi_j \rangle \right], \quad (5.21)$$

where

$$\begin{aligned} \langle \phi_i | \phi_j \rangle &= \sum_{\mu > \nu} \phi_{i\mu} \phi_{j\nu} n_{\nu\mu} \\ &= L \sum_{\mu > \nu} \phi_{i\mu} \phi_{j\nu}. \end{aligned} \quad (5.22)$$

The conclusion is that as $L \rightarrow \infty$ ($N \rightarrow \infty$) the phases oscillate very rapidly and the Feynman integrals are averaged to zero. This would not be the case, only if these phases cancel between themselves in a given Feynman diagram. As we will see this is just the case for planar diagrams.

Let us consider an arbitrary connected vacuum diagram with l loops. This diagram is necessarily one-particle irreducible because of the constraint $Q(0) = 0$. The Feynman rules are those of lattice fields Q_μ , $\bar{\eta}$, and ω with the phases (5.15) sitting at the vertices. If we use $Q(L - q)$ instead of $Q^*(q)$ in Eq. (5.17) the propagators will have phases as well:

$$\exp \left[\frac{2\pi i}{N} \langle k | k \rangle \right]. \quad (5.23)$$

To determine the overall phase factor corresponding to the diagram one can apply the following procedure.

(a) Cut l internal lines of the diagram to produce a connected tree diagram with $2l$ external lines [see Figs. 4(a) and 5(a)].

(b) Consider all vertices to be mediated by loops of an auxiliary field. The orientation of the loops is dictated by the ordering of

$$\text{Tr}[A(q_1) \cdots A(q_n)] \quad (5.24)$$

in the vertices.

(c) One can associate momenta χ to all lines of the auxiliary field in a fashion consistent with momentum conservation. The phase factor corresponding to any original vertex can be obtained by associating a phase factor to every new vertex of the field-fictitious-particle type. The prescription is as follows:

$$\exp \left[\frac{2\pi i}{N} \langle \chi_{\text{in}} | \chi_{\text{out}} - \chi_{\text{in}} \rangle \right], \quad (5.25)$$

where $\chi_{\text{in}, \text{out}}$ are the momenta of the incoming and outgoing fictitious particle. The momenta of the fictitious-particle lines are determined up to an

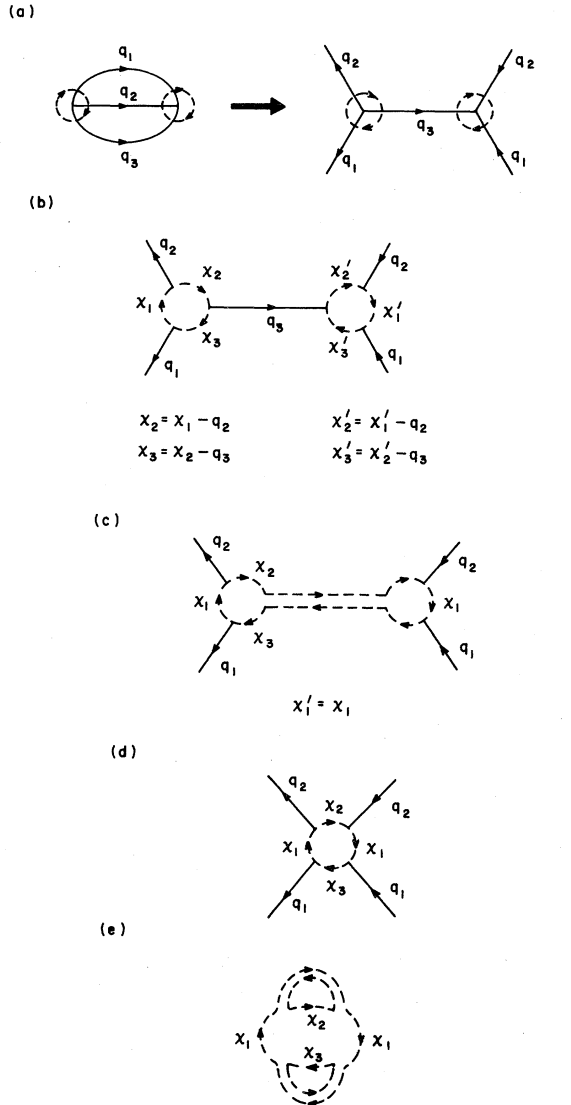


FIG. 4. Example of the procedure (a) to (e) to calculate the phase factor of a planar diagram. The arrows around the vertices specify the ordering of the traces:

$$\text{Tr}[A(q_1)A(q_2)A(q_3)]\text{Tr}[A(-q_1)A(-q_3)A(-q_2)].$$

The phase factor of this diagram is 1.

overall shift. This shift has no effect on the phase because the total momentum coming out of each vertex is zero [Figs. 4(b) and 5(b)].

(d) Using the freedom of shifting the overall momenta in each vertex it is possible to consider all internal lines as the independent propagation of two fictitious particles from one vertex to the other. This is shown in Figs. 4(c) and 5(c). Now, it is easy to see that the phase factors corresponding to internal propagators and vertices cancel completely.

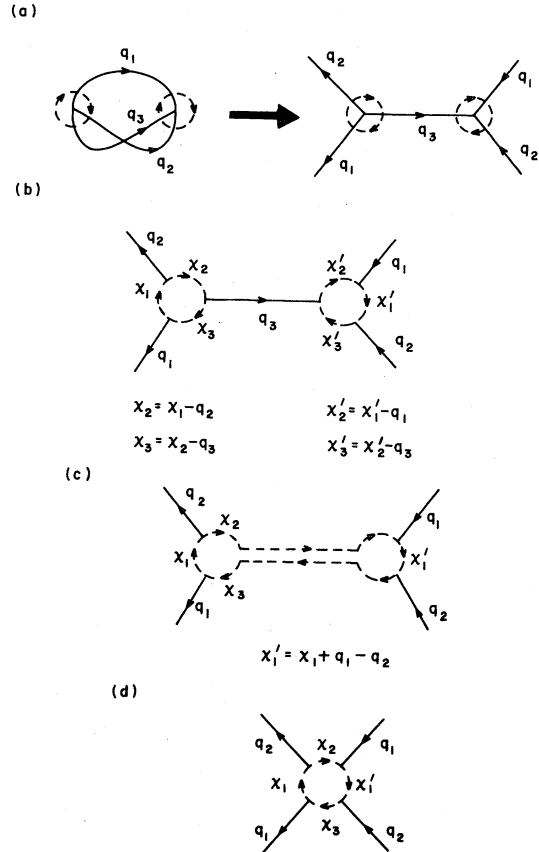


FIG. 5. Example of the procedure (a) to (d) to calculate the phase factor of a nonplanar diagram. The ordering in this case is

$$\text{Tr}[A(q_1)A(q_2)A(q_3)]\text{Tr}[A(-q_1)A(-q_2)A(-q_3)].$$

Substituting $A(q_i) \sim \lambda^{q_i}$ one can easily see how this diagram is nonplanar,

$$\sum_{a_1 a_2 a_3} \text{Tr}(\lambda^{a_1} \lambda^{a_2} \lambda^{a_3}) \text{Tr}(\lambda^{a_1} \lambda^{a_2} \lambda^{a_3}) \sim N$$

(instead of N^3). The phase factor of this diagram is given by

$$\exp \left[\frac{2\pi i}{N} \sum_{\mu, \nu} k_{i\mu} k_{j\nu} n_{\nu\mu} \right].$$

From one vertex one gets

$$\langle \chi_{in} | \chi_{out} - \chi_{in} \rangle. \tag{5.26}$$

On the other vertex the roles of in and out are exchanged and one gets

$$\langle \chi_{out} | \chi_{in} - \chi_{out} \rangle. \tag{5.27}$$

Adding them together one obtains

$$-\langle \chi_{in} - \chi_{out} | \chi_{in} - \chi_{out} \rangle \tag{5.28}$$

which is eliminated by the propagator phase.

(e) Since the phase factors of the internal propagators and vertices cancel each other, one can deform the diagram into a single vertex with $2l$ external lines. Half of the lines have momentum opposite to the other half [see Figs. 4(d) and 5(d)]. The final vertex is ordered (up to cyclic permutations) and the relative position of the momenta determines the final result. Planar diagrams are such that every external line with momentum q is adjacent to the line with momentum $-q$. In this case one can consider the external lines as composed of two independent propagators of the fictitious particle and reduce systematically all pairs of external lines with momentum q and $-q$ as in (d). [See Fig. 4(e).] The total phase of these diagrams cancel. Notice that this characterization of planar diagrams lies in the origin of Parisi's quenching prescription.¹⁸ It just reflects the fact that for a planar diagram the number of index loops equals the number of momentum loops plus one.

Finally, it is useful to give the remaining phase factor for any nonplanar diagram. One gets

$$\exp \left[\frac{\pi i}{N} \sum_{i,j} \epsilon_{ij} \sum_{\mu,\nu} k_{i\mu} k_{j\nu} n_{\nu\mu} \right], \quad (5.29)$$

where $\epsilon_{ij} = -\epsilon_{ji}$ is zero if between q_i and $-q_i$ there is either no q_j line or both lines. If the ordering is $q_i, q_j, -q_i, -q_j$, $\epsilon_{ij} = 1$ and for $q_j, q_i, -q_j, -q_i$ one obtains $\epsilon_{ij} = -1$.

As pointed out previously all nonplanar diagrams carry phases which oscillate very fast as $L \rightarrow \infty$ and the corresponding Feynman diagram yields a zero result. For a set of isolated points on the momentum integration region the phases might cancel, but this is always a region of zero measure and does not alter our conclusion.

An interesting remark allows us to reinterpret the fact that the vacuum energy is proportional to N^2 . In our construction it is a statement of the well-known fact that the vacuum energy is proportional to the volume of space-time $L^4 = N^2$.

To conclude, we mention that our result can be generalized to any matrix model in the adjoint representation. For this purpose one starts applying our prescription (5.3) to the action. The rest of the proof applies equally well to this case.

VI. NUMERICAL ANALYSIS

In this section we study the TEK model numerically by performing Monte Carlo simulations. The calculational procedure employed here is described in Ref. 15.

We first check whether the vacuum expectation

values of open Wilson loop vanish. In the SU(16) gauge group ($L = 4$) we evaluated

$$W_{k_\mu}(C) = \frac{1}{N} \text{Tr}(U_0^{k_0} U_1^{k_1} U_2^{k_2} U_3^{k_3}) \quad (6.1)$$

for all k_μ satisfying $L > k_0 \geq k_1 \geq k_2 \geq k_3 \geq 0$ except $k_\mu = 0$ ($\mu = 0, \dots, 3$). Throughout the whole range of coupling constants the real and imaginary parts of $W_{k_\mu}(C)$ fluctuate only in the interval ± 0.1 . We do not see any indication of the $[U(1)]^d$ symmetry breaking. For example in Fig. 6 we show $(1/N)\langle \text{Tr} U_0 \rangle$ as a function of β/N . Each point is an average over 25 iterations. Other open Wilson loops behave in the same way.

In Fig. 7 we plot $(1/N)\text{Tr} U_0$ at $\beta/N = 0.4$ for several gauge groups $SU(L^2)$, $L = 4, 5, 6$, and 7, starting from the initial configuration Eq. (4.17). As L increases fluctuations of $(1/N)\text{Tr} U_0$ become small. Notice that in our twist configuration (4.16), $Z_{\mu\nu}$ approaches to 1 in the large- N limit. Figure 7 shows, however, that in this limit the minimum-action configuration $U_\mu^{(0)}$ becomes stable. Although $Z_{\mu\nu}$ approaches to 1, the excitation state $U_\mu = 1$ cannot contribute to the partition function. Substituting $U_\mu = 1$ in Eq. (2.10), we have the excitation energy of this configuration as

$$\beta N d (d - 1) (1 - \cos 2\pi/L) \quad (6.2)$$

which diverges as $N \rightarrow \infty$ with β/N fixed.

Figure 8 shows the internal energy

$$E = \frac{1}{12N} \left\langle \sum_{\mu \neq \nu} Z_{\mu\nu} U_\mu U_\nu U_\mu^\dagger U_\nu^\dagger \right\rangle \quad (6.3)$$

of the TEK model as a function of β/N . We used the SU(16) group. Each point is an average over 50~100 iterations. In the strong- and weak-coupling regions, the data agree very well with the curves of the leading terms in the strong- and weak-coupling expansions of the standard Wilson theory.

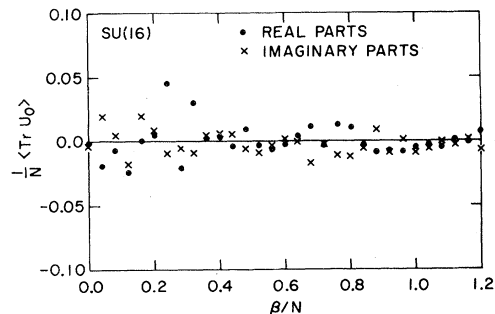


FIG. 6. The Monte Carlo data of $(1/N)\langle \text{Tr} U_0 \rangle$ for gauge group SU(16). Each point is an average of 25 iterations.

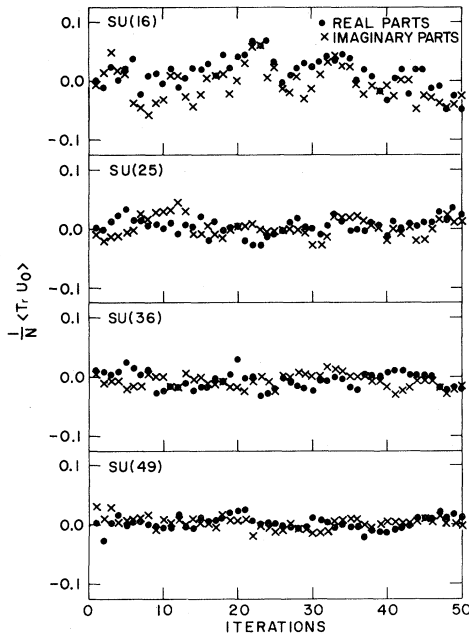


FIG. 7. The data of $(1/N)\text{Tr}U_0$ at $\beta/N=0.4$ for several gauge groups $SU(L^2)$, $L=4, 5, 6$, and 7 .

The model has the same phase structure as the large- N limit of the Wilson theory.²⁹ It undergoes a first-order phase transition. Latent heats are observed near $\beta/N=0.35\sim 0.36$. We also study the model for the $SU(25)$ group. We observed a latent heat near $\beta/N=0.36$. Figure 9 shows the result of two long runs at this point with disordered and twisted initial conditions. Notice that the values of critical coupling does not depend crucially on the gauge groups $SU(16)$ and $SU(25)$. It seems that our model approaches to the $N\rightarrow\infty$ limit very fast.

Finally we evaluate the χ ratio

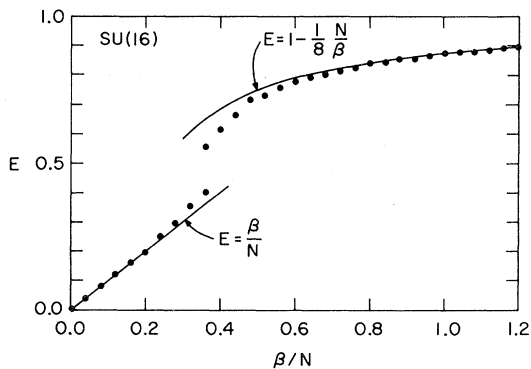


FIG. 8. The internal energy of the TEK model as a function of β/N . The curves are the leading terms of the strong- and weak-coupling expansion for Wilson's theory.

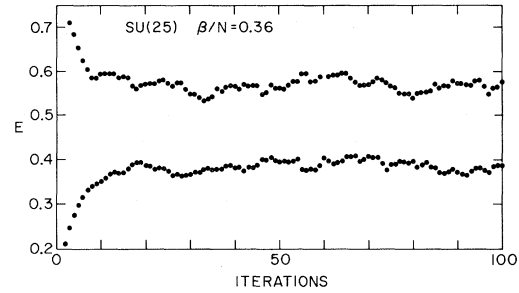


FIG. 9. Two Monte Carlo runs at $\beta/N=0.36$ with disordered and twisted initial conditions.

$$\chi(I,J) = -\ln \frac{W(I,J)W(I-1,J-1)}{W(I,J-1)W(I-1,J)}, \quad (6.4)$$

where $W(I,J)$ is a rectangular Wilson loop of dimension I and J . $W(I,J)$ is calculated using the formula (2.25). We use the $SU(36)$ group which corresponds to the usual Wilson theory of the 6^4 lattice. Figure 10 shows $W(I,J)$ up to $I=J=3$. It is difficult to measure larger Wilson loops in the strong-coupling region because they become very small. In Fig. 11 we plot the χ ratio (6.4). $\chi(1,1)$ are read from Fig. 8. The dashed lines in the weak-coupling region represent the corresponding χ ratio of the usual $U(3)$ Wilson theory on the 6^4 lattice.³⁰ Our data fit well to these curves.

In the critical region fluctuations of $W(I,J)$ are very big. It is difficult to determine the scale of the Λ parameter from our present data. More detailed study of this region is currently under investigation.

VII. CONCLUDING REMARKS

In the previous sections the TEK model has been studied in several regions of the coupling constant and using different techniques. In addition to the equivalence of the loop equations, the study of its

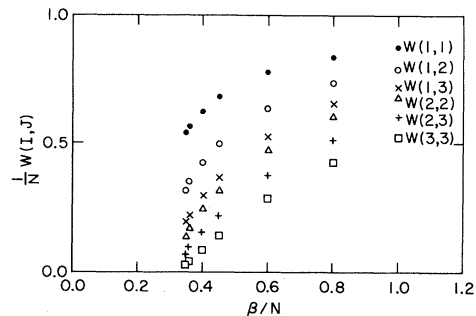


FIG. 10. Wilson loops as a function of β/N for the $SU(36)$ gauge group. Each point is an average over 20–40 iterations.

strong-coupling and weak-coupling expansion shows the validity of this model as a reduced version of the infinite-lattice Wilson theory. Further support comes from the Monte Carlo data which show no sign of $[U(1)]^d$ symmetry breaking at intermediate coupling. The internal energy and χ ratios have the expected features of their infinite-lattice counterparts.

Our analysis has also shown the leading finite- N corrections. At strong coupling they are basically of the same size as for the EK model. In the weak-coupling region they correspond to the finite-size effects on an $(\sqrt{N})^4$ lattice. In this respect, the TEK model seems to approach the $N \rightarrow \infty$ limit faster than the QEK model. The finite- N corrections of the latter correspond to the finite-size effects on an $(N^{1/4})^4$ lattice as shown by Alfaro and Sakita.²²

The TEK model is also simpler compared to other reduced models at large N . From a numerical point of view it only requires the same computer time as the EK model for the same value of N . From an analytical point of view it seems better suited for nonperturbative studies.

Another possible check comes from the two-dimensional case. As mentioned previously the exact solution is known for the large- N infinite-lattice Wilson theory.⁶ It is worthwhile to point out that in this case the usual Eguchi-Kawai model is probably valid as well,¹⁴ since $[U(1)]^d$ symmetry breaking occurs only for $d > 2$. Goldschmidt³⁴ has claimed that the Eguchi-Kawai model reproduces the result

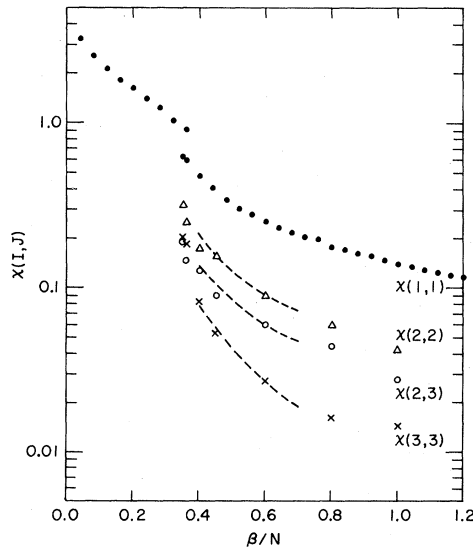


FIG. 11. The χ ratios of the TEK model. $\chi(1,1)$ is read from Fig. 8. The dashed lines represent the corresponding χ ratio of the usual $U(3)$ Wilson theory on the 6^4 lattice.

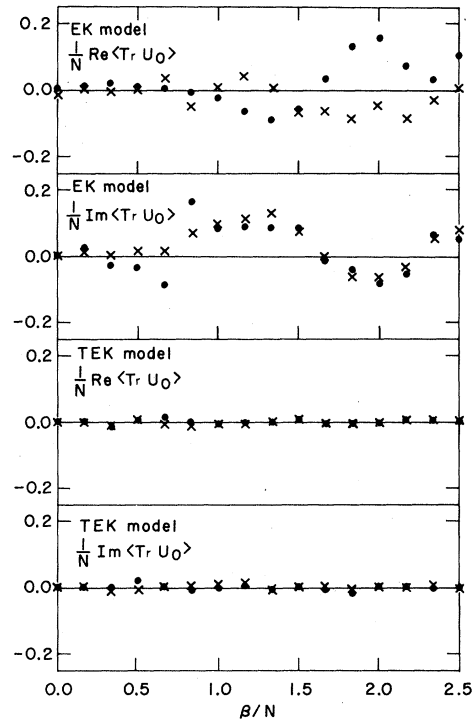


FIG. 12. The Monte Carlo data of $(1/N)\langle \text{Tr} U_0 \rangle$ for two-dimensional EK and TEK models in the rapid thermal cycles. The crosses and dots represent heating and cooling, respectively. Each point is an average of 50 iterations.

of Gross and Witten in the $N \rightarrow \infty$ limit. It is simple to see that the same proof applies to the TEK model.

To give some numerical evidence in this direction we performed Monte Carlo simulations of the two-dimensional EK and TEK models. In Fig. 12 we show $(1/N)\langle \text{Tr} U_0 \rangle$ as functions of β/N . Our twist configuration is chosen to be $n_{01} = 4$ and the gauge

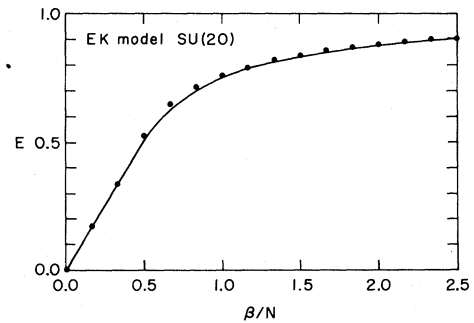


FIG. 13. The internal energy of the two-dimensional EK model as a function of β/N . The solid line is a theoretical prediction (7.1).

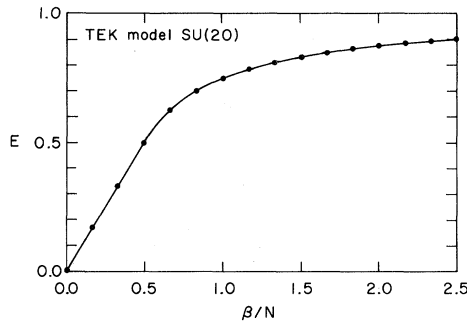


FIG. 14. The internal energy of the two-dimensional TEK model.

group is SU(20). Although in both EK and TEK models $\langle \text{Tr}U_\mu \rangle$ is zero, fluctuations are large in the EK model.

Figures 13 and 14 show the results of the internal energy compared to the prediction⁶

$$\begin{aligned} E(\beta) &= \frac{\beta}{N}, & \frac{\beta}{N} \leq \frac{1}{2}, \\ E(\beta) &= 1 - \frac{1}{4} \frac{N}{\beta}, & \frac{\beta}{N} \geq \frac{1}{2}. \end{aligned} \quad (7.1)$$

The data agree nicely with the theoretical expectations in the TEK model. In the EK model the data are slightly above the line (7.1). Probably this is due to the big fluctuation of $\text{Tr}U_\mu$.

It is also useful to compare the result of larger Wilson loops. For an $I \times J$ Wilson loop the prediction is given by

$$\frac{1}{N} \langle W(I, J) \rangle = \left(\frac{\beta}{N} \right)^{IJ}, \quad \frac{\beta}{N} \leq \frac{1}{2}, \quad (7.2)$$

$$\frac{1}{N} \langle W(I, J) \rangle = \left[1 - \frac{1}{4} \frac{N}{\beta} \right]^{IJ}, \quad \frac{\beta}{N} \geq \frac{1}{2}.$$

In the TEK model, comparison of this prediction with the data is given in Table II. We use the SU(30) gauge group and $n_{01}=6$. For EK model we obtain qualitatively the same result. However, fluctuations are so big that it is difficult to extract a meaningful χ ratio of larger Wilson loops.

To conclude this section let us state some of the problems which deserve some study in the future. It is tempting to believe that the simplicity of the TEK model will allow analytical solutions for large N . At least, it is possible that rigorous results can be established on the behavior of large Wilson loops and the issue of confinement. From a numerical standpoint it would be good to obtain continuum quantities from the TEK model; in particular, the value of the string tension and the meson spectrum. These results will show how far the SU(3) values are from the $N \rightarrow \infty$ ones. These points are currently under investigation by the authors.

ACKNOWLEDGMENTS

The authors have profitted from many interesting discussions with their colleagues at BNL, Mike Creutz, Herbert Hamber, and Claudio Rebbi. We also acknowledge useful discussions and correspon-

TABLE II. Wilson loops and χ ratios for the two-dimensional TEK and EK models. Data are averaged over 200–300 iterations. The theoretical prediction is given in Eq. (7.2).

	TEK data	$\beta/N=0.25$ theory	TEK data	$\beta/N=0.5$ theory	TEK data	$\beta/N=1.0$ theory	TEK data	$\beta/N=1.5$ theory	EK data	$\beta/N=1.5$ theory
$\frac{1}{N} W(1,1)$	0.249	0.25	0.501	0.5	0.747	0.75	0.835	0.833	0.841	0.833
$\frac{1}{N} W(1,2)$	0.061	0.063	0.250	0.25	0.556	0.563	0.698	0.694	0.705	0.694
$\frac{1}{N} W(1,3)$	0.013	0.016	0.124	0.125	0.413	0.422	0.584	0.579	0.597	0.579
$\frac{1}{N} W(2,2)$	0.001	0.004	0.061	0.063	0.304	0.316	0.489	0.482	0.501	0.482
$\frac{1}{N} W(2,3)$			0.021	0.016	0.168	0.178	0.344	0.335	0.371	0.335
$\frac{1}{N} W(3,3)$					0.065	0.075	0.203	0.194		
$\chi(2,2)$			0.719	0.693	0.306	0.288	0.176	0.182	0.166	0.182
$\chi(2,3)$					0.299	0.288	0.173	0.182	0.132	0.182
$\chi(3,3)$					0.347	0.288	0.179	0.182		

dence with T. Eguchi, J. Groeneveld, C. P. Korthals Altes, B. Sakita, P. van Baal, and K. Wilson. One of us (A.G.-A) wants to thank the High Energy Theory Group at BNL for the hospitality extended

to him.

This work was supported in part by the U.S. Department of Energy under Contract No. DE-AC02-76CH00016.

*Permanent address: Departamento de Fisica Teorica C-X1, Universidad Autonoma de Madrid, Cantoblanco, Madrid, Spain.

¹G. 't Hooft, Nucl. Phys. B72, 461 (1974).

²K. Wilson, Phys. Rev. D 10, 2445 (1974).

³This proof has been shown for the massive case, and not yet for the massless case. G. 't Hooft, Phys. Lett. 109B, 474 (1982); Commun. Math. Phys. 86, 449 (1982).

⁴G. 't Hooft, Phys. Lett. 119B, 369 (1982); Commun. Math. Phys. 88, 1 (1983).

⁵G. 't Hooft, Nucl. Phys. B75, 461 (1974).

⁶D. Gross and E. Witten, Phys. Rev. D 21, 446 (1980).

⁷E. Brezin, C. Itzykson, G. Parisi, and J. B. Zuber, Commun. Math. Phys. 59, 35 (1978).

⁸A. A. Migdal, Ann. Phys. (N.Y.) 126, 279 (1980).

⁹E. Witten, *Recent Developments in Field Theory* (Plenum, New York, 1980).

¹⁰Y. M. Makeenko and A. A. Migdal Phys. Lett. 88B, 135 (1979).

¹¹T. Eguchi and H. Kawai, Phys. Rev. Lett. 48, 1063 (1982).

¹²D. Foerster, Phys. Lett. 87B, 87 (1979); Nucl. Phys. B170, 107 (1980); T. Eguchi, Phys. Lett. 87B, 91 (1979); D. Weingarten, *ibid* 87B, 97 (1979).

¹³G. Bhanot, U. M. Heller, and H. Neuberger, Phys. Lett. 113B, 47 (1982).

¹⁴A. Gonzalez-Arroyo, J. Jurkiewicz, and C. P. Korthals Altes, in *Proceedings of the 1981 Freiburg NATO Summer Institute* (Plenum, New York, 1982).

¹⁵M. Okawa, Phys. Rev. Lett. 49, 353 (1982).

¹⁶G. Bhanot, U. M. Heller, and H. Neuberger, Phys. Lett. 115B, 237 (1982).

¹⁷M. Okawa, Phys. Rev. Lett. 49, 705 (1982).

¹⁸G. Parisi, Phys. Lett. 112B, 463 (1982).

¹⁹S. Das and S. Wadia, Phys. Lett. 117B, 228 (1982); G. Parisi and Y. C. Zhang, Phys. Lett. 114B, 319

(1982).

²⁰T. Eguchi and H. Kawai, University of Tokyo report, 1982 (unpublished).

²¹D. Gross and Y. Kitazawa, Nucl. Phys. B206, 440 (1982).

²²J. Alfaro and B. Sakita, Phys. Lett. 121B, 339 (1983); U. M. Heller and H. Neuberger, Nucl. Phys. B207, 399 (1982).

²³I. Bars, Phys. Lett. 116B, 57 (1982); J. Greensite and M. B. Halpern, Nucl. Phys. B211, 343 (1983); G. Maiella and P. Rossi, CERN Report No. TH-3416, 1982 (unpublished); U. M. Heller and H. Neuberger, Phys. Rev. Lett. 49, 621 (1982); G. Bhanot, Phys. Lett. 120B, 371 (1983).

²⁴T. L. Chen, C.-I. Tan, and X. T. Zheng, Phys. Lett. 116B, 419 (1982); A. A. Migdal, *ibid* 116B, 425 (1982).

²⁵A. Gonzalez-Arroyo and M. Okawa, Phys. Lett. 120B, 174 (1983).

²⁶G. 't Hooft, Nucl. Phys. B153, 141 (1979).

²⁷J. Groeneveld, J. Jurkiewicz, and C. P. Korthals Altes, Phys. Scr. 23, 1022 (1981).

²⁸G. 't Hooft, Commun. Math. Phys. 81, 267 (1981).

²⁹M. Creutz, Phys. Rev. Lett. 46, 1441 (1981).

³⁰M. Creutz and K. J. M. Moriarty, Nucl. Phys. B210 [FS6], 377 (1982).

³¹P. van Baal, Commun. Math. Phys. 85, 529 (1982).

³²J. Ambjørn and H. Flyvbjerg, Phys. Lett. 97B, 241 (1980).

³³B. E. Baaquie, Phys. Rev. D 16, 2612 (1977); A. Hasenfratz and P. Hasenfratz, Nucl. Phys. B193, 210 (1981); R. Dashen and D. J. Gross, Phys. Rev. D 23, 2340 (1981); H. Kawai, R. Nakayama, and K. Seo, Nucl. Phys. B189, 40 (1981); P. H. Weisz, Phys. Lett. 100B, 331 (1981); A. Gonzalez-Arroyo and C. P. Korthals Altes, Nucl. Phys. B205, 46 (1982).

³⁴Y. Y. Goldschmidt, Phys. Lett. 119B, 174 (1982).